Synthesis of Gold Nanoparticles in Hyperbranched Polyol Dispersions

Zhiliang Zhang,[1] Chongqi Shou[2]

[1]*Research Center of Analysis and Test, Shandong Institute of Light Industry, Jinan 250353, China*
[2]*College of Chemistry and Chemical Engineering, University of Jinan, Jinan 250022, China*

Received 16 December 2010; accepted 18 February 2011
DOI 10.1002/app.34343
Published online 29 June 2011 in Wiley Online Library (wileyonlinelibrary.com).

ABSTRACT: In this study, a series of different generation hyperbranched poly(amine-ester) with hydroxyl as terminal group were synthesized and used as protectants to synthesize gold nanoparticles with a facile and highly reproducible method. The effect of hyperbranched poly (amine-ester) generation on size and their distribution of gold nanopartciels were discussed. The results of ultraviolet visible absorption spectroscopy, Transmission electron microscopy and scanning electron microscopy showed that the mean diameter were 24.3 ± 2.6 nm, 18.2 ± 2.1 nm, and 13.6 ± 1.5 nm corresponding to the different generation hyperbranched poly(amine-ester), and the synthesized gold nanoparticles were almost monodisperse with a narrow size distribution. © 2011 Wiley Periodicals, Inc. J Appl Polym Sci 122: 2849–2854, 2011

Key words: gold nanoparticles; narrow size distribution; hyperbranched polyols dispersion

INTRODUCTION

Attractive for their size, stability, and biocompatibility, gold nanoparticles have received much attention in various potential applications fields since the last two decades.[1] They can be widely used in a variety of fields, including drug delivery,[2] biological sensoring,[3] electrochemistry[4] biofuel cell,[5] catalysis,[6] nonlinear optical switching,[7] immunoassays,[8,9] surface plasmon,[10] photonics,[11] and surface-enhanced Raman scattering (SERS).[12,13] As a result, research is emphasized on developing a series of effective methodologies to synthesize gold nanoparticles in recent years. Most of the methods are proceeded in solution based chemical techniques such as chemical reduction,[14] sonochemical reduction,[15] polyol process,[16] radiolytic reduction,[17] and photochemical reduction.[18]

To control the size and polydispersity of nonaparticles with the methods mentioned above, different kinds of organic small molecule and macromolecules were used as stabilizers, such as thiols and their derivatives,[19,20] polyaniline,[21] polyvinylpyrrolidone,[22] C60,[23] ciprofloxacin,[24] poly(ethylene oxide)-poly(propylene oxide)-poly(ethylene oxide) block copolymer,[25] paclitaxel,[26] alkanetelluroxide,[27] alkylamine,[28] and so on. The stabilizing effects of these molecules are attributable to the fact that either the small particles were attached to the much larger protecting polymers or the protecting molecules covered the metal particles. Using dendrimers to tailor metal nanoparticles have also been gaining attention in the recent past years.[29] They are considered to be good candidates for preparing functional nanoparticles for their unique properties.[30,31] Firstly, dendritic branches and terminal groups are effective to control the access of small substrates into the dendrimers and thus to obtain nanaoparicles with a narrow size distribution. Secondly, the loose steric aspects of dendrimers also allow the encapsulated nanoparticles to participate in various catalytic reactions, and the terminal groups on the dendrimer periphery can be modified for purposes of nanoparticle solubility in different media.[32] Therefore, dendrimers are excellent stabilizer for generating metal functional nanoparticles. However, the synthesis and characterization of dendrimers are very difficult and costly, which severely limit dendrimers application in the synthesis of metal functional nanoparitcles.

In comparison to the cost-intensive and time-consuming multistep synthesis of dendrimers, hyperbranched polymers can be obtained by a single-step in large quantity and are commercially available in industrial quantities.[33] Moreover, hyperbranched polymers have similar molecular structure and properties with dendrimers, which could be a new kind of potential candidates for synthesis of nanoparticles. To date, several kind of hyperbranched polymers has been used as protectants to prepare metal

Correspondence to: Z. Zhang (zhangzhiliang0531@163.com).

Contract grant sponsor: Shandong Province Municipal Major Science and Technology; contract grant number: 2006GG1108097-10.

nanoparticles, such as silver nanoparticles, but they are seldom used to synthesize gold nanopatticles.[34–37] Following our previous study on hyperbranched polymer,[38–40] we reported here a successful synthesis method of gold nanoparticles with different generation hyperbranched poly(amine-ester) as proctectants. According to review of the literature available to us, hyperbranched poly(amine-ester) with pentaerythritol as core (HPAE) has been not used to synthesize gold nanoparticles. In this article, a series of different generation HPAE were synthesized, and used to synthesize gold nanoparticles with a facile and highly reproducible one-pot method by reducing gold ions with D-glucose. The effect of the HPAE generation on gold nanoparticles size and their distribution were investigated, and the role of the HPAE during the synthesis process was also discussed.

EXPERIMENTAL

Reagents and apparatus

Apparatus

Fourier transform infrared (FTIR) spectra in the range of 400–4000 cm^{-1} were recorded on FTIR TENSOR 27 (Bruker, Germany). The liquid sample was dropped onto a KBr pellet and covered with another KBr pellet and all measurements were performed in transmittance mode at 2 cm^{-1} resolution. ^{1}HNMR spectrum was collected on a Bruker AV400 spectrometer (Bruker AXS, Germany) using CD_3OD as solvent. Elemental analysis was conducted on a VARIO ELIII elemental analyses meter (VARIO, Germany). GPC was performed with Waters 1525 Binary HPLC Pump using Waters 2414 refractive index detector, Styragel HT 2,3,4 as columns, and THF as eluant. UV-Vis spectra of samples were recorded in a Hitachi (U-4100, Tokyo, Japan) UV-Vis spectrophotometer. X-ray diffraction studies were made on the powder samples at room temperature on a D8 X-ray diffractometer (Bruker, Germany). The scanning rate used was 5.0° min^{-1} over the range of 2θ = 10–90°C. The TEM images were obtained with JEM-1010 transmission electron microscope (JEOL, Japan) at 60 kV. The samples were prepared by placing two or three drops of the dilute gold nanoparticles dispersion in alcohol on carbon-coated copper grids. The SEM images were investigated by Quanta200 scanning electron microscopy (FEI, Holland). The samples of SEM were prepared by dispersing the final nanoparticles in ethanol; the dispersion was then dropped on silicon wafer. Size distribution and number-average particle diameters were obtained using the Image ProPlus Image Analysis System.

Materials

Methyl methacrylate, 2,2′-dihydroxydiethylamine and pentaerythritol, were purchased from Sigma-Aldrich Co. (St. Louis, America). Chloroauric acid, D-glucose and *p*-toluene sulfonic acid were obtained from Alfa Aesar Co. (Karlsruhe, Gemany). The other chemicals were analytical or high-reagent grade.

Synthesis of hyperbranched poly(amine-ester) with pentaerythritol as core

The *N*,*N*-diethylol-3-amine methylpropionate was synthesized according to the literature.[41] The 0.5 mol methyl acrylate, 0.5 mol diethanolamine, and 50 mL methanol were added into a 100-mL three-necked flask, the admixture was stirred at 35°C for 4 h, then removed the methanol by vacuumizing and *N*,*N*-diethylol-3-amine methylpropionate was obtained.

Pentaerythritol(0.1 mmol), *N*,*N*-diethylol-3-amine methylpropionate (2.8 mmol), and *p*-toluene sulfonic acid (0.015 mmol) were added into a three-necked flask. The mixture were heated to 120°C and kept for 2 h on the temperature. The methanol formed in the synthesis process was removed from the mixture by vacuumizing, and ether was added into the mixture to remove *p*-toluene sulfonic acid. After these treatments, the final product was the third generation (G3) of HPAE with pentaerythritol as core, where Gn referred to the generation number. When the molar ration of pentaerythritol and *N*,*N*-diethylol-3-amine methylpropionate were 1 : 60 and 1 : 124′ with the same synthesis method, the forth and fifth generation(G4 and G5) of HPAE with pentaerythritol as core were received, respectively. The synthesis scheme of HPAE with pentaerythritol as core was shown in Figure 1.

N,*N*-diethylol-3-amine methylpropionate, IR (KBr, ν, cm^{-1}), 3248 (—OH), 2932, 2852 ($—CH_2$), 1733 (—C=O), 1302, 1035 (—C—O—), 1200 (C—N). ^{1}HNMR (CD_3OD, 400 MHz, δ ppm): 3.635 (CH_3—O—), 2.446 (O=C—CH_2—CH_2—), 2.786 (O=C—CH_2—CH_2—), 2.575 (—*N*—CH_2—CH_2—), 3.550 (—*N*—CH_2—CH_2—), 3.339 (—O*H*). Elemental analysis of *N*,*N*-diethylol-3-amine methylpropionate (%): C (49.88), H (9.26), N (7.58).

G3, G4, and G5 HPAE, IR (KBr, ν, cm^{-1}), G3: 3552-3250 (—OH), 1739(C=O), 1304, 1035 (C—O), 876 ($—OCH_2$), 2935, 2856, 1440 ($—CH_2$—), 1201 (—C—N). G4: 3560-3260 (—OH), 1738 (C=O), 1306, 1035 (C—O), 876 ($—OCH_2$), 2936, 2855, 1443 ($—CH_2$—), 1205 (—C—N). G5: 3562-3263 (—OH), 1740 (C=O), 1312, 1036 (C—O), 881 ($—OCH_2$), 2936, 2856, 1446 ($—CH_2$—), 1208 (—C—N). ^{1}HNMR (CD_3OD, 400 MHz, δ ppm), G3: 4.24 (—*N*—CH_2—CH_2O*H*), 3.36, 3.12 (—*N*—CH_2C*H*$_2$OH), 2.69 (—*N*—CH_2CH_2OH), 2.62 ($—CH_2$—O—CO—CH_2C*H*$_2$—), 2.35, 2.32 ($—CH_2$—O—CO—CH_2CH_2—), 3.51 ($—CH_2$—O—CO—CH_2CH_2—), 1.19

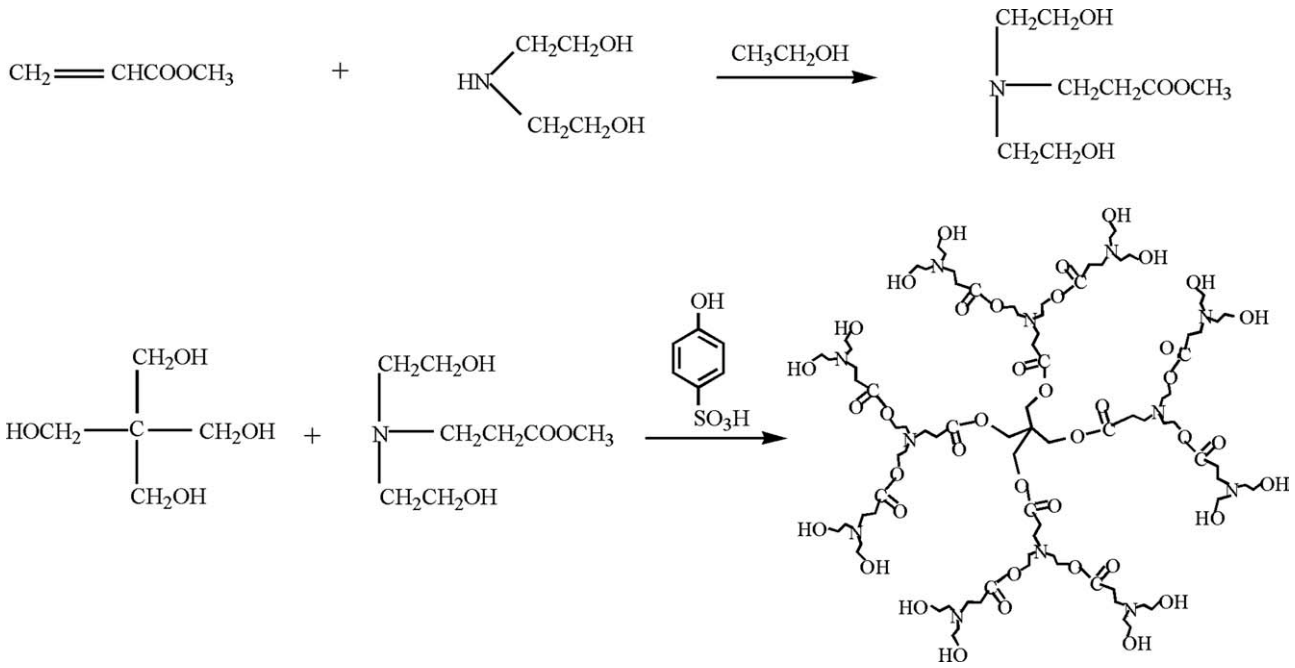

Figure 1 The synthesis scheme of HPAE with pentaerythritol as core.

(—CH_2—). G4:4.28 (—N—CH_2—CH_2OH), 3.40, 3.16 (—N—CH_2CH_2OH), 2.72 (—N—CH_2CH_2OH), 2.61 (—CH_2—O—CO—CH_2CH_2—), 2.38, 2.34 (—CH_2—O—CO—CH_2CH_2—), 3.56 (—CH_2—O—CO—CH2CH2—), 1.21 (—CH_2—). G5:4.31 (—N—CH_2—CH_2OH), 3.36, 3.14 (—N—CH_2CH_2OH), 2.70 (—N—CH_2CH_2OH), 2.59 (—CH_2—O—CO—CH_2CH_2—), 2.42, 2.38 (—CH_2—O—CO—CH_2CH_2—), 3.51 (—CH_2—O—CO—CH_2CH_2—), 1.22 ppm (—CH_2—). Molecular weight and polydispersity of HPAE (M_w, PDI), G3:1.565 × 10^3, 3.28; G4: 3.672 × 10^3, 3.56; G5: 6.562 × 10^3 3.82. Hydroxyl value of HPAE (mg KOH/g), G3: 379; G4: 375; G5: 369.

Preparation gold nanoparticles encapsulated with HPAE

Gold nanoparticles encapsulated with G3 HPAE were prepared by a very simple method. In a typical synthesis process, 20 mL aqueous solution containing 60 mg chloroauric acid was slowly added into a beaker containing 120 mg G3 HPAE in 20 mL aqueous solution in alkaline environment. The mixture was stirred for 30 min to form Au-HPAE complex. Next, the complex was reduced by slow addition of 20 mL aqueous solution containing 128 mg D-glucose. After fixed period of reaction, the gold nanoparticles were separated form the solution by vigorous centrifugation at 20,000 rpm for 15 min to remove any excess protect agents, and redispersed D.I. water. By these treatments, gold nanoparticles encapsulated G3 HPAE were obtained. The gold nanoparticles with G4 and G5 HPAE were received, respectively, with the same synthetic procedure.

RESULTS AND DISCUSSION

UV-Vis spectra of gold nanoparticles encapsulated with HPAE

The UV-Vis spectra of gold nanoparticles encapsulated with different generation of HPAE were shown in Figure 2. It displayed a strong absorption at around 520 nm, which arose from the surface plasmon absorption. According to Mie's theory,[42] the position and shape of the adsorption peaks were affected by the nature of the metal nanoparticles,

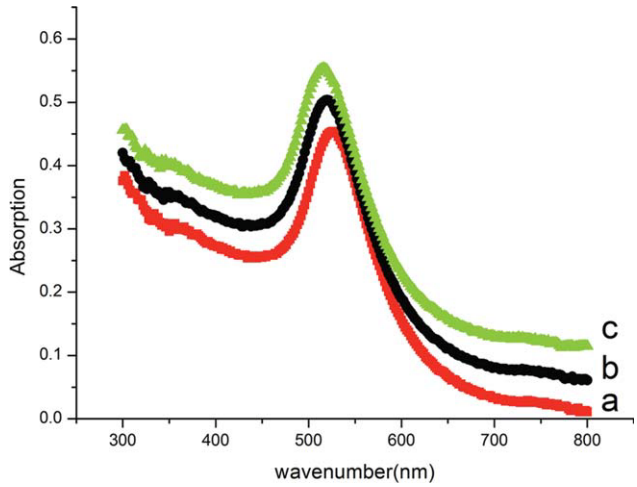

Figure 2 UV-Vis spectra of gold nanoparticles encapsulated with G3 HPAE (526 nm, curve a), G4 HPAE (523 nm, curve b), and G5 HPAE (519 nm, curve c), respectively. [Color figure can be viewed in the online issue, which is available at wileyonlinelibrary.com.]

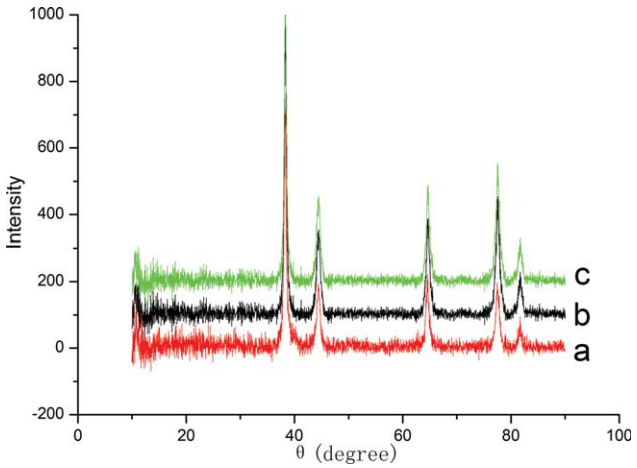

Figure 3 XRD spectra of gold nanoparticles encapsulated with G3 HPAE (curve a), G4 HPAE (curve b), and G5 HPAE (curve c), respectively. [Color figure can be viewed in the online issue, which is available at wileyonlinelibrary.com.]

such as size, shape, and the status of aggregation. Compared the absorption spectra in Figure 2, the peak positions for curves a, b, and c was determined to be at 526, 523, and 519 nm, corresponding to gold nanoparticles encapsulated with G3, G4, and G5 HPAE, respectively. The peak was shifted toward red on decreasing the HPAE generation which suggested that there were the bigger gold nanoparticles to form in the synthesis system,[43,44] and these results were in good agreement with the later TEM and SEM analysis.

XRD spectra of gold nanoparticles encapsulated with HPAE

The crystalline structure of the synthesized gold nanoparticles encapsulated with G3, G4, and G5 HPAE were examined by electron and X-ray diffraction and shown in Figure 3(a–c), respectively. X-ray diffraction analysis showed peaks (111) at $2\theta = 38.2^\circ$, (200) at $2\theta = 44.4^\circ$, (220) at $2\theta = 64.7^\circ$, (311) at $2\theta = 77.7^\circ$, and (222) at $2\theta = 81.4^\circ$ which matched the literature values of gold nanoparticles.[45] All the reflection peaks at about 38.2, 44.4, 64.7, 77.7, and 81.4° can be indexed to face-centered cubic crystal structure representing the 111, 200, 220, 311, and 222 Braggs reflections. The results provided supporting evidence for the HPAE-encapsulated crystal structure and confirmed the formation of gold nanoparticles.[46]

TEM and SEM of gold nanoparticles encapsulated with HPAE

TEM micrographs of synthesized gold nanoparticles encapsulated with G3, G4, and G5 HPAE were presented in Figure 4(a–c), and their SEM micrographs were displayed in Figure 4(d–f), respectively. As shown in Figure 4, all gold nanoparticles exhibited regular spherical shape homogeneously with respect to the morphology. The analysis of gold nanoparticles synthesized using G3 HPAE indicated that most of them were in the size range of 21–27 nm [Fig. 4(a,d)]. When G4 HPAE was employed, it produced spherical nanoparticles in the size range 15–21 nm [Fig. 4(b,e)]. Using G5 HPAE, the

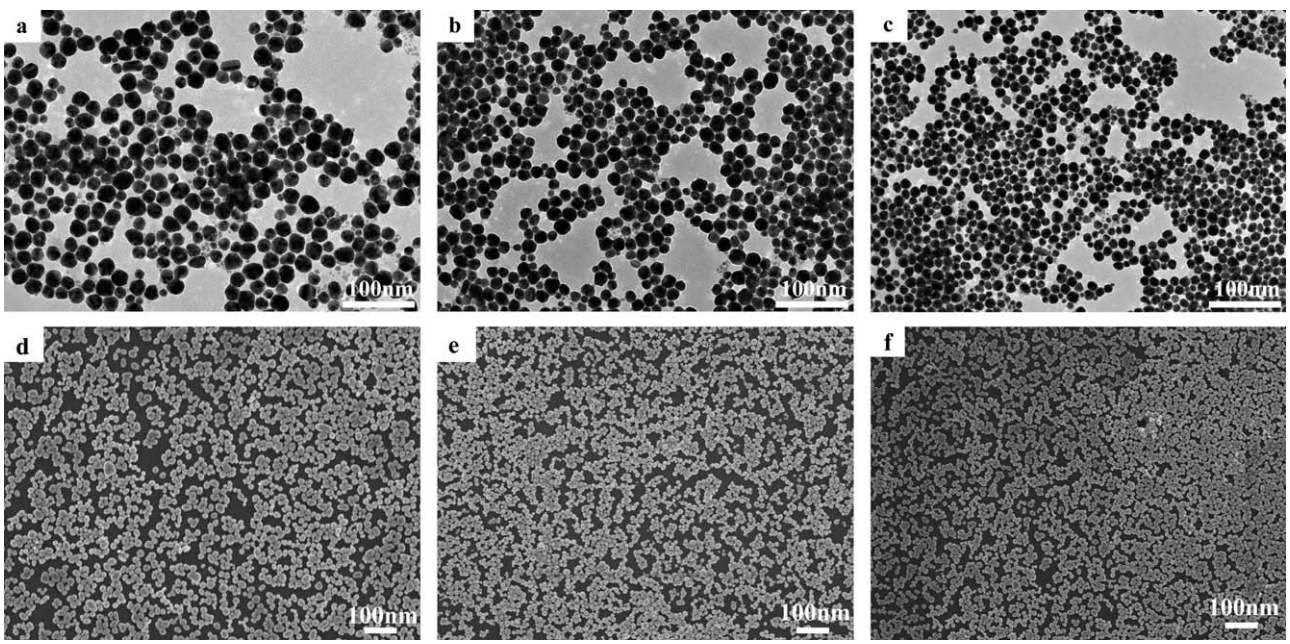

Figure 4 TEM and SEM of gold nanoparticles encapsulated with G3 HPAE (a,d), G4 HPAE (b,e), and G5 HPAE (c,f), respectively.

TABLE I
The Characteristic Data of Gold Nanopartiles Encapsulated with HPAE

Generation	$HAuCl_4$/HPAE (mm)	λ_{max} (nm)	Mean nanoparticles size (nm)	Standard deviation
G3	1 : 2	526	24.3	±2.6
G4	1 : 2	523	18.2	±2.1
G5	1 : 2	519	13.6	±1.5

nanoparticles size decreased in the range 11–16 nm [Fig. 4(c,f)]. These changes in gold nanoparticle size, dependent on the HPAE generation, were in good agreement with the UV-Vis spectra presented above. When no protectants were added into the reaction system following the same synthesis procedure, the synthesized particles aggregated and the particles size was several microns, or even tens of microns. Moreover, the shape of synthesized particles was irregular. These results suggested that HPAE could effectively prevent the synthesized particles from aggregation.

Compared TEM and SEM images in Figure 4, the characteristic data in Table I clearly demonstrated that the mean size of the synthesized gold nanoparticles decreased from 24.3 ± 2.6 to 13.6 ± 1.5 nm with the generation of HPAE increase. From Table I, it was also noteworthy that the standard deviation of the synthesized gold nanoparticles decreased with the generation of HPAEA increase. It was evident from above that the HPAE generation played an important role in the synthesis of gold nanoparticles. From TEM, SEM, and Table I, the synthesized gold nanoparticles had a narrow particle distribution, almost monodisperse. It may be concluded that HPAE could efficiently prevent gold nanoparticles from aggregation during the synthesis process and may be perfect protectants to synthesize metal nanoparticles.

An understanding of the mean nanoparticles size and standard deviation change with HPAE generation increase could now be obtained by examining the process involved in the buildup to gold nanoparticles. It has been postulated that metal ions could bind with the atom at the surface and interior of the HPAE, the gold nanoparticles formation would generally take place in the internal cavity of HPAE molecules or among the HPAE molecules. When G3 HPAE molecules were used, the internal cavities were bigger and the steric effect was smaller. As the structure evolved to G4 HPAE molecule, the internal environment started to get defined, more so in G5 HPAE molecule, creating smaller cavities around the central pentaerythritol core. Moreover, the steric effect of G4 and G5 HPAE molecules was higher compared with G3 HPAE molecules and could prevent gold nanoparticles from aggregation to form bigger nanoparicles. At the same time, the terminal groups of HPAE molecules increased rapidly with the generation increase, and were very effective to stabilize the gold nanoparticles by binding with the gold nanoparticles. From mentioned above, it was reasonable that the mean nanoparticles size and standard deviation became smaller with HPAE generation increase.

TABLE II
The $HAuCl_4$/HPAE Mass Ratio Effect on the Mean Size and Distribution

Generation	$HAuCl_4$/HPAE (mm)	λ_{max} (nm)	Mean nanoparticles size (deviation	
G4	1 : 1	527	26.1	±3.7
G4	1 : 2	523	18.2	±2.1
G4	1 : 3	520	15.3	±1.9

The $HAuCl_4$/HPAE mass ratio effect on the mean size and distribution were also investigated, and the results were shown in the Table II. From the Table II, the mean size and distribution decreased with the $HAuCl_4$/HPAE mass ratio increase. The mean size of the synthesized gold nanoparticles decreased from 26.1 ± 3.7 to 15.3 ± 1.9 nm as the $HAuCl_4$/HPAE mass ratio increased from 1 : 1 to 1 : 3. From Table II, it was also shown that the standard deviation of the synthesized gold nanoparticles decreased. This was because there were more protectants to prevent the synthesized gold nanoparticles from aggregating with the $HAuCl_4$/HPAE mass ratio increase, and monodisperse gold nanoparticles were obtained.

CONCLUSION

In summary, different generation HPAE with hydroxyl as terminal group were synthesized and used to synthesize gold nanoparticles with a facile and highly reproducible method. The mean diameter of synthesized gold nanoparticles encapsulated with G3, G4, and G5 HPAE were 24.3 ± 2.6 nm, 18.2 ± 2.1 nm, and 13.6 ± 1.5 nm, respectively. From the UV-Vis spectra, TEM and SEM images, the synthesized gold nanoparticles capsulated with HPAE molecules were almost monodisperse, which proved that HPAE were a new kind of perfect protectants to synthesize metal nanoparticles. This method successfully provided a facile way to synthesize uniform and functional gold nanoparticles.

References

1. Li, G.; Li, D.; Zhang, L.; Zhai, J.; Wang, E. Chem Eur J 2009, 15, 9868.
2. Cheng, Y.; Samia, A. C.; Meyers, J. D.; Panagopoulos, I.; Fei, B.; Burda C. J Am Chem Soc 2008, 130, 10643.

3. Zhang, T.; Wang, W.; Zhang, D.; Ma, Y.; Zhou, Y.; Qi, L. Adv Funct Mater 2010, 20, 1152.
4. Murata, K.; Kajiya, K.; Nukaga, M.; Suga, Y.; Watanabe, T.; Nakamura, N.; Ohno. H. Electroanalysis 2010, 22, 185.
5. Murata, K.; Kajiya, K.; Nakamur, N.; Ohno, H. Energy Environ Sci 2009, 2, 1280.
6. Wang, X.; Li, G.; Chen, T.; Yang, M.; Zhang, Z.; Wu, T.; Chen, H. Nano Lett 2008, 8, 2643.
7. Venkatram, N. K.; Santosh, R. S.; Rao, N.; Medda, D; De, S. K. J Nanosci Nanotechnol 2006, 6, 1990.
8. Liu, B. H.; Tsao, Z. J.; Wang, J. J.; Yu, F. Y. Anal Chem 2008, 80, 7029.
9. Cui, R.; Liu, C.; Shen, J.; Gao, D.; Zhu, J.; Chen, H. Y. Adv Funct Mater 2008, 18, 2197.
10. Gifford, L. K.; Sendroiu, I. E.; Corn, R. M.; Lupta, A. J Am Chem Soc 2010, 132, 9265.
11. Yamaguchi, H.; Matsuda, K. Chem Lett 2009, 38, 946.
12. Alexander, K. D.; Hampton, M. J.; Zhang, S.; Dhawan, A.; Xu, H.; Lopez, R. J Raman Spectrosc 2009, 40, 2171.
13. Dasary, S. S. R.; Singh, A. K.; Senapati, D.; Yu, H.; Ray, P. C. J Am Chem Soc 2009, 131, 13806.
14. Bhargava, S. K.; Booth, J. M.; Agrawal, S.; Coloe, P.; Kar, G. Langmuir 2005, 21, 5949.
15. Jin, Y.; Wang, P.; Yin, D.Liu, J.; Qin, L.; Yu, N.; Xie, G.; Li, B. Colloid Surf A Physicochem Eng Aspect 2007, 302, 366.
16. Abargues, R.; Gradess, R.; Canet-Ferrer, J.; Abderrafi, K.; Valde'sa, J. L.; Martı'nez-Pastora, J. New J Chem 2009, 33, 913.
17. Plech, A.; Kotaidis, V.; Siems, A.; Sztucki, M. Phys Chem Chem Phys 2008, 10, 3888.
18. Eustis, S.; Hsu, H. Y.; El-Sayed, M. A. J Phys Chem B 2005, 109, 4811.
19. Grumelli, D.; Vericat, C.; Benitez, G.; Vela, M. E.; Salvarezza, R. C. J Phys Chem C 2007, 111, 7179.
20. Dass, A.; Guo, R.; Tracy, J. B.; Balasubramanian, R.; Douglas, A. D.; Murray, R. W. Langmuir 2007, 24, 310.
21. Zheng, G. X.; Shao, Y.; Xu, B. Acta Chim Sin 2006, 64, 733.
22. Yan, N.; Zhang, J.; Yuan, Y.; Chen, G. T.; Dyson, P. J.; Li, Z. C.; Kou, Y. Chem Commun 2010, 46, 1631.
23. Brust, M.; Kiely, C. J.; Bethell, D.; Schiffrin, D. J. J Am Chem Soc 1998, 120, 12367.
24. Tom, R. T.; Suryanarayanan, V.; Reddy, P. G.; Baskaran, S.; Pradeep, T. Langmuir 2004, 20, 1909.
25. Sakai, T.; Alexandridis, P. J Phys Chem B 2005, 109, 766.
26. Gibson, J. D.; Khanal, B. P.; Zubarev, E. R. J Am Chem Soc 2007, 129, 11653.
27. Li, Y.; Silverton, L. C.; Schlenoff, J. B. Langmuir 2008, 24, 7048.
28. Wang, X.; Xu, S.; Zhou, J.; Xu, W. J Colloid Interface Sci 2010, 348, 24.
29. Sutton, A.; Franc, G.; Kakkar, A. J Polym Sci Polym Chem 2009, 47, 4482.
30. Hourani, R.; Whitehead, M. A.; Kakkar, A. K. Macromolecules 2008, 41, 508.
31. Franc, G.; Kakkar, A. K.; Chem Commun 2008, 42, 5267.
32. Sardar, R.; Funston, A. M.; Mulvaney, P.; Murray, R. W. Langmuir 2009, 25, 13840.
33. Gladitz, M.; Reinemann, S.; Radusch, H. J Macromol Mater Eng 2009, 294, 178.
34. Liu, S. H.; Qian, X. F.; Yin, J.; Hong, L.; Wang, X. L.; Zhu, Z. K. J Solid State Chem 2002, 168, 259.
35. Lu, H. W.; Liu, S. H.; Wang, X. L.; Qian, X. F.; Yin, J.; Zhu, Z. K. Mater Chem Phys 2003, 81, 104.
36. Zhu, Z.; Kai, L.; Wang, Y. Mater Chem Phys 2006, 96, 447.
37. Mahapatra, S. S.; Karak, N. Mater Chem Phys 2008, 112, 1114.
38. Shou, C.; Zhou, C.; Zhao, C.; Zhang, Z.; Li, G.; Chen, L. Talanta 2004, 63, 887.
39. Shou, C.; Zhang Z. J Appl Polym Sci 2009, 111, 2141.
40. Shou, C.; Song, N.; Zhang Z. J Appl Polym Sci 2010, 116, 2473.
41. Lu, Y.; Lin, D.; Wei, H. Y.; Shi, W. F. Acta Polym Sin 2000, 4, 411.
42. Mie, G. Ann Phys 1908, 25, 377.
43. Schofield, C. L.; Haines, A. H.; Field, R. A.; Russell, D. A. Langmuir 2006, 22, 6707.
44. Li, G.; Luo, Y. Tan, H. J Solid State Chem 2005, 178, 1038.
45. Kar, T.; Dutta, S.; Das, P. K. Soft Matter 2010, 6, 4777.
46. Radziuk, D.; Grigoriev, D.; Zhang, W.; Su, D.; Mohwald, H.; Shchukin, D. J Phys Chem C 2010, 114, 1835.